

**DEVELOPMENT AND CHARACTERIZATION OF THE IONIC POLYMER  
METAL COMPOSITE ACTUATED CONTRACTILE WATER JET  
THRUSTER**

**by**

**MUHAMMAD FARID BIN SHAARI**

**Thesis submitted in fulfilment of the  
requirements for the degree  
of Doctor of Philosophy**

**February 2017**

## **ACKNOWLEDGEMENTS**

First of all I would like to express my gratefulness to Allah the Almighty which make me able to finish this project successfully. I would like to dedicate my sincere gratitude and thankful to my supervisor, Associate Professor Dr. Zahurin bin Samad who had supervised me along this time. His passions, guidance and continuous support for this project had led to the accomplishment of my studies. His efforts are muchly appreciated. Secondly, I would like to thank all the supporting staffs, Mr. Norijas Abd. Aziz, Mr. Mohd Ali Shabana Mohd Raus, Mr. Mohd Ashamuddin Hashim, Mr. Hashim Md. Nordin and Mr. Rosnin Saranor who had guided me in dealing with technical stuffs as well as procurement process as well as to all my colleagues; Dr. Cham Chin Long, Mr. Muhammad Alif Rosly, Mr. Muhammad Husaini Abu Bakar, Mr. Lim Chong Hooi and Mr. Ameer Mohamed Abdeel Aziz Mohamed Hanafee who had spent time together in sharing the knowledge and finding the solutions.

I am also would like to thank and address my appreciation to Malaysian Government for providing the IPTA Academic Training Scheme (SLAI) scholarship and Universiti Sains Malaysia for financial support of this project under the Exploratory Research Grant Scheme (ERGS) 2011 (Grant no.: 203/PMEKANIK/6730008). Finally I would like to thank my beloved wife for her continuous support and great sacrifices, my children who always inspired me to complete my studies and also to my family for their supports and prayers. Alhamdulillah.

## TABLE OF CONTENTS

	Page
<b>ACKNOWLEDGEMENTS</b>	ii
<b>TABLE OF CONTENTS</b>	iii
<b>LIST OF TABLES</b>	vii
<b>LIST OF FIGURES</b>	viii
<b>LIST OF ABBREVIATION</b>	xiii
<b>LIST OF SYMBOLS</b>	xv
<b>ABSTRAK</b>	xviii
<b>ABSTRACT</b>	xix
 <b>CHAPTER ONE: INTRODUCTION</b>	
1.1 Background	1
1.2 Problem Statement	5
1.3 Objectives	7
1.4 Scope of Work	7
1.5 Organization of Thesis	8
 <b>CHAPTER TWO: LITERATURE REVIEW</b>	
2.1 Squid mantle morphology and propulsion system	9
2.2 AUV propulsion system	13
2.3 CWJT	18
2.3.1 Contraction frequency	19
2.3.2 Thrust and drag	20
2.3.3 Dimensionless parameter	24
2.3.4 Previous works on CWJT	26
2.4 Smart material actuators	34
2.5 IPMC actuator	40

2.5.1	Factors that influence IPMC performance	43
2.5.2	Overview on IPMC actuator fabrication	46
2.5.3	Overview on IPMC actuator characterization	48
2.6	Summary of literature review	50
 <b>CHAPTER THREE: METHODOLOGY</b>		
3.1	IPMC actuator development	52
3.1.1	IPMC fabrication	52
3.1.2	IPMC actuator characterization	58
3.2	CWJT prototype design	65
3.2.1	Conceptual design	66
3.2.2	CWJT mantle model determination	68
3.2.3	Drag experimental procedure	75
3.2.4	Drag simulation procedure	76
3.2.5	CWJT detail design	81
3.3	CWJT prototype fabrication	83
3.4	Ejected fluid flow simulation	85
3.5	CWJT contraction measurement	88
3.5.1	Volume differentiation measurement procedure	89
3.5.2	Volume contraction calculation	91
3.6	Empirical thrust measurement	94
3.6.1	Experimental setup	94
3.6.2	Experiment procedure	96
3.7	Summary	98

## **CHAPTER FOUR: RESULTS AND DISCUSSION**

4.1	IPMC actuator characterization result	100
4.1.1	IPMC actuator force characterization results	100
4.1.2	IPMC actuator's oscillation characterization results	105
4.2	CWJT Prototype Design	107
4.2.1	CWJT model	107
4.2.2	Drag analysis	109
4.3	Fluid flow simulation analysis	113
4.3.1	Pressure distribution	116
4.3.2	Velocity distribution	120
4.3.3	Generated thrust	125
4.4	CWJT contraction analysis	126
4.4.1	Contraction displacement	127
4.4.2	Contraction volume	132
4.5	Empirical thrust measurement	135
4.5.1	Water jet velocity measurement	135
4.5.2	Water jet thrust	138

## **CHAPTER FIVE: CONCLUSION AND RECOMMENDATION**

5.1	Research conclusion	143
5.2	Research contribution	146
5.3	Recommendation and future works	147

<b>REFERENCES</b>	149
-------------------	-----

## **APPENDICES**

Appendix A: Nafion specification

Appendix B: Simulation results of mantle model deformation

Appendix C: AUV orthographic drawing

Appendix D: CWJT Drawings

Appendix E: AUV velocity and shear wall stress simulation

Appendix F: Water jet dynamic pressure and total pressure simulation

Appendix G: Water jet velocity contour simulation

Appendix H: Water jet velocity vector simulation

Appendix I: Arduino programming code

Appendix J: Thrust calculation

## **LIST OF PUBLICATIONS**

## LIST OF TABLES

	<b>Page</b>
Table 2.1 Previous research on the CWJT	31
Table 2.2 Classification of smart material actuators	35
Table 2.3 Characteristics of actuators and its definition	38
Table 2.4 The displacement and driving force of IPMC at different DC supply voltages of 1V-3V (Chung et al., 2006)	44
Table 3.1 LDPE properties (Plasticintl, 2016)	71
Table 3.2 Mesh models for mantle model grid independency test	73
Table 3.3 Mesh models for AUV drag grid independency test	79
Table 3.4 Control Parameters and AUV Dimension	81
Table 3.5 Mechanical Properties for EVA copolymer	84
Table 3.6 Mesh models for fluid velocity grid independency test	86
Table 3.7 Actuation frequency	91
Table 4.1 DOE analysis to verify the most influential factors on the displacement the IPMC actuator during oscillation	108
Table 4.2 Simulation results for all design models	110
Table 4.3 Averaging the contraction displacement highest (frequency)	128
Table 4.4 Averaging the contraction displacement (lowest frequency)	129
Table 4.5 Compilation of averaged data for every frequency and nozzle aperture diameter	129
Table 4.6 Angle for every contraction in radian	133
Table 4.7 Contraction volume of for every samples	134
Table 4.8 Water jet velocity	137

## LIST OF FIGURES

	<b>Page</b>
Figure 1.1      Classification of Swimming Mechanism (Colgate and Lynch, 2004)	3
Figure 2.1      Squid morphology (Krieg and Mohseni, 2010)	10
Figure 2.2      Squid mantle muscles and its structure (Gosline and De Mont, 1985)	10
Figure 2.3      a) The parallel lines present squid radial muscle and (b) SEM image of complex collagen fibres in squid mantle	11
Figure 2.4      Contractile phases of the squid mantle (Gosline and De Mont, 1985)	12
Figure 2.5      Variation of commercial thrusters. From left, open rotary propeller blade on the right is the water jet thruster	14
Figure 2.6      Some examples of AUV thrusters (Lin and Guo, 2012; Gonzalez, 2004. (a) Centrifugal thrusters with nozzle, (b) rotary blade propeller	15
Figure 2.7      Underwater vehicle or robot propulsion system classification.	16
Figure 2.8      Examples of bio-inspired propulsion system; Robosquid (Krueger et al., 2010) and Vortex ring thruster (Krieg and Mohseni, 2009)	17
Figure 2.9      Fundamental concept of the contractile water jet propulsion; (a) Relax phase, (b) Inflation phase and (c) Deflation phase	19
Figure 2.10     Acting forces for a moving AUV	21



Figure 2.11	Bollard Pull Test (Muljowidodo et al., 2009); a) Schematic diagram b) Actual test	23
Figure 2.12	Thrust measurement using gage test (Guo et al., 2010)	24
Figure 2.13	Vortex ring formation based on formation number (Gharib et al., 1998); a) $L/D = 2$ , b) $L/D = 3.8$ and c) $L/D = 14.5$	26
Figure 2.14	Speed per body length performance of several underwater biomimetic propulsion system (Chu et al., 2012)	27
Figure 2.15	Comparison of CWJT locomotion speed performance with other propulsion systems and its natural counterparts (Chu et al., 2012)	29
Figure 2.16	Work capacity of smart material actuators according to their weight (Zupan et al., 2002)	39
Figure 2.17	Basic IPMC actuator structure	41
Figure 2.18	Nafion (perfluorinated alkene) monomer	41
Figure 2.19	IPMC actuation phase (Punning et al., 2007); (a) IPMC without voltage supply, (b) IPMC with voltage supply	42
Figure 2.20	IPMC model (Shahinpoor and Kim, 2001)	43
Figure 2.21	IPMC actuation free body diagram (Ji et al., 2009)	44
Figure 2.22	Designation of every dimension for IPMC actuator (Ji et al., 2009)	46
Figure 2.23	IPMC displacement at different thickness and supply voltage (Kim et al., 2003)	47
Figure 2.24	IPMC tip force at different thickness and supply voltage (Kim et al., 2003)	47
Figure 2.25	IPMC actuation induced by AC voltage supply	50
Figure 2.26	Schematic diagram for characterization setup (Vahabi et al., 2011)	50

Figure 3.1	Primary process to fabricate the IPMC (Yu et al., 2007; Yip et al., 2011)	54
Figure 3.2	Platinum salt hydrate ( $[\text{Pt}(\text{NH}_3)_4]\text{Cl}_2$ )	55
Figure 3.3	Reduction process in water bath	55
Figure 3.4	Flow chart for the secondary process (Yu et al., 2007; Yip et al., 2011)	57
Figure 3.5	Platinum particles formed on the Nafion surface during reduction process and became grey coloured IPMC	58
Figure 3.6	Pictorial view of the actuating force characterization	61
Figure 3.7	Schematic of actuation force characterization	61
Figure 3.8	Oscillation characterization with illustrated laser beam for displacement measurement.	63
Figure 3.9	Schematic of oscillating characterization	64
Figure 3.10	AUV Prototype with CWJT Thruster	66
Figure 3.11	Real squid mantle	67
Figure 3.12	Conceptual design of the proposed CWJT	67
Figure 3.13	Force elements during contraction	69
Figure 3.14	Proposed CWJT mantle designs	70
Figure 3.15	Flow chart for the simulation analysis	72
Figure 3.16	Definition of the fixed support area and the deformable area of the model at specific actuation force magnitude	74
Figure 3.17	AUV rapid prototype for drag test	75
Figure 3.18	Drag testing experimental setup	76
Figure 3.19	Simulation process flow for ANSYS Fluent software	78
Figure 3.20	The AUV size and fluid domain ratio	79

Figure 3.21	Meshed domain	80
Figure 3.22	Setting the boundary condition in ANSYS Fluent	81
Figure 3.23	Design of the mould for CWJT mantle	85
Figure 3.24	Geometrical model of the simulation	87
Figure 3.25	Example of calculation and converged solution	88
Figure 3.26	Experimental setup for contraction measurement	90
Figure 3.27	Actual contraction measurement	90
Figure 3.28	3D view of the contraction volume of the CWJT	92
Figure 3.29	Area division to determine the volume by integration	93
Figure 3.30	Experimental setup schematic diagram	95
Figure 3.31	Actual setup test rig	95
Figure 3.32	Ejection time, $t_e$ calculation	98
Figure 4.1	Supply voltage influence on actuation the force characterization	101
Figure 4.2	Metal plated influence on the actuation force characterization	102
Figure 4.3	IPMC actuator force characterization at different thickness	104
Figure 4.4	IPMC actuator force characterization at different length and orientation of actuation	105
Figure 4.5	Displacement of IPMC actuator at different length and input frequency	107
Figure 4.6	Grid independency test for the CWJT mantle model	110
Figure 4.7	Grid independency test for shear wall stress of the AUV	111
Figure 4.8	Drag analysis via simulation and experiment	113
Figure 4.9	Drag contour based on fluid flow velocity	114
Figure 4.10	Grid independency test for fluid flow analysis	115
Figure 4.11	The relation between Total Pressure, Dynamic Pressure and	117

	Static Pressure at various nozzle aperture	
Figure 4.12	Dynamic pressure distribution in the nozzle and at the opening	119
Figure 4.13	Total pressure distribution within the nozzle and at the opening	119
Figure 4.14	Dynamic and total pressure for different nozzle aperture diameter at 10 mm water jet trail	120
Figure 4.15	Fluid velocity analysis using ANSYS FLUENT software	121
Figure 4.16	Vector analysis on fluid flow	122
Figure 4.17	Relation between fluid velocity and the nozzle aperture diameter	125
Figure 4.18	Thrust at different nozzle aperture size by simulation result	126
Figure 4.19	Acquisition of raw data for the highest actuation frequency, 0.5 Hz	127
Figure 4.20	Acquisition of raw data for the lowest actuation frequency, 0.005 Hz	128
Figure 4.21	The correlation between displacement and actuation frequency at different nozzle apertures	130
Figure 4.22	Determination of affected zone to measure the maximum contraction volume	132
Figure 4.23	Contraction volume at different actuation frequency	135
Figure 4.24	Fluid ejection during contraction	136
Figure 4.25	Measurement of the water jet velocity	136
Figure 4.26	Water jet velocity and the nozzle aperture sizes	137
Figure 4.27	Thrust at different nozzle aperture	139
Figure 4.28	Comparison between the experiment and simulation thrust	142

## LIST OF ABBREVIATIONS

AC	Alternating current
ANOVA	Analysis of Variance
ASTM	American Society for Testing and Materials
AUV	Autonomous Underwater Vehicle
BCA-O	Body/Caudal Actuation-Oscillatory
BCA-U	Body/Caudal Actuation-Undulatory
CAD	Computer Aided Design
CFD	Computational Fluid Dynamic
CNT	Carbon nanotube
CP	Conductive polymer
CWJT	Contractile water jet thruster
DAQ	Data acquisition
DC	Direct current
DE	Dielectric elastomer
DI	Deionized water
DOE	Design of Experiment
DOF	Degree of Freedom
DPIV	Digital Particle Image Velocimetry
EAP	Electro active polymer
EVA	Ethylene Vinyl Acetate
EW	Equivalent weight
FDM	Fused Deposition Modelling
FEA	Finite Element Analysis
gf	Gram force

IPMC	Ionic Polymer Metal Composite
JET	Water jet propulsion
MPA-O	Median/Paired Actuation-Undulatory
MPA-U	Median/Paired Actuation-Oscillatory
PTFE	Polytetrafluoroethylene
ROV	Remotely operated vehicle
SEM	Scanning electron microscope
SMA	Shape memory alloy

## LIST OF SYMBOLS

$\frac{\partial V}{\partial t}$	Volume changes in time
$\mu$	Dynamic viscosity of the fluid
$A_{AUV}$	Fluid-AUV contact area
$A_c$	Contact area of the actuator on the CWJT
$A_n$	Nozzle aperture
BL/s	Speed unit in Body-Length per second
$C_D$	Drag coefficient
$C_T$	Capacitive ion transduction
$D_n$	Nozzle diameter
$E$	Young Modulus
$eq$	Ion exchange capacity
$EW$	Equivalent weight
$\mathcal{E}_0$	Lever deformation
$F_B$	Blocking force
$F_b$	Reaction force from the body of the CWJT
$f_c$	Contraction frequency
$F_c$	Contraction/Actuation force
$F_D$	Drag force
$f_i$	Input frequency
$F_{wj}$	Reaction force from the contraction
Hz	Frequency unit, Hertz
$h$	IPMC thickness
$I$	Second moment inertia
$k_b$	Constant of CWJT body

$L$	IPMC actuator length
$L/D$	Length over diameter ratio
$L_e$	Maximum distance of the ejected fluid
$L_l$	Length of the force to the strain gage
$L_n$	Length of the nozzle channel
$m_e$	Ejected fluid mass
$\dot{m}_e$	Mass flow rate of the ejected fluid
$m_i$	Initial fluid mass
$p$	Distributed load of the IPMC
$P_{act}$	Actuation pressure (Applied pressure by IPMC on CWJT)
$P_c$	Contraction pressure (inside CWJT)
$P_s$	Static pressure
$P_T$	Total pressure
$q$	Dynamic pressure
$Q$	Fluid volumetric flowrate
$Re$	Reynolds number
$R_h$	Hydrodynamic resistance
$R_n$	Nozzle radius
$R_p$	Resistance across the Nafion
$R_s$	Resistance between electrode and Nafion
$R_{ss}$	Surface resistance of the IPMC
$S$	IPMC actuator bending displacement
$S_{max}$	Maximum IPMC actuator bending displacement
$T$	Oscillation period
$t_c$	Contraction time



$t_e$	Time taken to reach the maximum distance of the ejected fluid
$T_f$	Thrust
$u_b$	AUV velocity
$u_j$	Average jet velocity
$V_c$	Contraction volume or ejected fluid volume (mm <sup>3</sup> ) at certain time
$V_s$	Supply voltage (v)
$V_{max}$	Maximum contraction volume (mm <sup>3</sup> )
$\dot{V}_f$	Contraction volume rate
$v_{AUV}$	AUV velocity
$v_e$	Ejected fluid velocity
$v_i$	Initial fluid velocity
$\nu_k$	Kinematic viscosity of water
$\nu_{osc}$	Oscillation speed
$W$	Width of the contraction volume
$w$	Width of IPMC actuator
$Z$	Moment second area
$Z_w$	Nafion induction
$\alpha$	IPMC actuator bending angle
$\beta$	CWJT contraction angle
$\delta$	CWJT mantle displacement
$\Delta P$	Pressure drop
$\pi$	pi (3.142)
$\rho_f$	Fluid density
$\rho_w$	Water density
$\bar{y}$	Distance between centroid of affected zone and the axis of rotation

# **PEMBANGUNAN DAN PENCIRIAN PENUJAH JET AIR MENGECEUT GERAKAN KOMPOSIT POLIMER – LOGAM BERION**

## **ABSTRAK**

Komposit Polimer-Logam Berion (IPMC) merupakan salah satu bahan pintar yang boleh digunakan sebagai penggerak untuk Penujah Jet Air Mengecut (CWJT) yang merupakan penujah jet air alternatif untuk kenderaan bawah air berautonomi (AUV). Kelebihan penggerak IPMC adalah ianya ringan, fleksibel, boleh digunakan dalam air dan memerlukan voltan yang rendah. Walaubagaimanapun daya gerak IPMC yang rendah menghadkan penjanaan daya tujah. Oleh demikian, kajian ini dijalankan untuk menyiasat sifat aliran bendalir yang terhasil daripada gerakan IPMC ke atas CWJT. Siasatan ini meliputi pemerhatian terhadap hubungkait di antara beberapa faktor yang mempengaruhi penghasilan daya tujah seperti saiz muncung jet, bekalan tenaga untuk IPMC dan frekuensi gerakan IPMC. Kajian ini melibatkan kerja-kerja merekabentuk konsep prototaip penujah, fabrikasi dan mencirikan penggerak IPMC, simulasi keadaan bendalir pada rekabentuk prototaip dan juga beberapa ujikaji untuk penentusahan data. Hasil ujikaji dan penentusahan data menunjukkan saiz muncung jet dan frekuensi penggerak merupakan faktor utama dalam pembangunan penujah jet air yang digerakkan oleh IPMC. Frekuensi penggerak yang sesuai adalah di bawah 0.1 Hz. Sebarang nilai frekuensi melebihi 0.1 Hz akan mengurangkan keupayaan pengecutan CWJT. Daya tujahan maksima yang dicapai dalam penyelidikan ini adalah 4.52 mN pada bekalan kuasa sebanyak 6 V. Ini tidak sesuai untuk AUV yang berat dan mempunyai panjang lebih dari 1 m. Walau bagaimanapun, ia sesuai untuk AUV kecil atau AUV mikro yang beroperasi dalam air yang berarus rendah.

**DEVELOPMENT AND CHARACTERIZATION OF THE IONIC POLYMER  
METAL COMPOSITE ACTUATED CONTRACTILE WATER JET  
THRUSTER**

**ABSTRACT**

Ionic Polymer Metal Composite (IPMC) is a type of smart material that can be utilized as the actuator for contractile water jet thruster (CWJT) which is an alternative thruster for autonomous underwater vehicle (AUV). The advantages of IPMC actuator are light, flexible, able to be utilized underwater and consuming low voltage. However, IPMC low actuation force has limited the thrust generation. Hence, this research had been conducted to investigate the character of the fluid flow generated by the IPMC actuation on the CWJT. This investigation includes the observation on the relation of few factors that influence the thrust generation such as the nozzle aperture size, supply voltage for IPMC actuation and actuation frequency. This research consists of designing the conceptual prototype thruster, fabricating and characterizing the IPMC actuator, simulating the fluid flow of the prototype design and few experiments for data validation. The results and validation from the experiments showed that nozzle aperture size and actuation frequency of the IPMC actuator were influential factors in the development of IPMC actuated CWJT. The feasible actuation frequency was 0.1 Hz. Any higher frequency than 0.1 Hz would decline the CWJT contraction performance. The maximum thrust achieved in this research was 4.52 mN at 6 V supply. It is not feasible for heavy and more than 1 m long AUV. However, it suits for small or micro AUV that works in low current waters.

# **CHAPTER ONE**

## **INTRODUCTION**

### **1.1 Background**

The development of autonomous underwater vehicle (AUV) is simply driven by three major lines of motivation; the underwater biodiversity exploration, environmental ecology concern and the current fast growing sub-ocean industry (Yuh, 2000b; Roper et al., 2010). The related task that requires AUV service regarding these domain of activities including underwater research, oil and gas exploration, underwater construction, water quality monitoring, military activities, sub-ocean mining and eco-tourism. The working environment and nature of the task has determined the design of the AUV. For instance, a linear motion seabed topography scanning requires a torpedo shape AUV design for minimal drag influence. On the other hand, three dimensional seabed pipeline monitoring would utilize a 6 Degree of Freedom (DOF) box shaped AUV design because it has more manoeuvrability and linear speed locomotion is not a priority (Guo et al., 2010; Shi et al., 2013). Meanwhile, Yue et al. (2015) and Guo et al. (2016) had designed and developed a spherical AUV which has the advantage in manoeuvrability, flexibility and outstanding shock resistance.

One of the current trend in the AUV development and has become great attention from many researchers is the small scale AUV that is able to do sensing and observation tasks in various dimension and complex structure (Curtin et al., 2005; Lin and Guo, 2012). In addition, by applying swarm AUV sensing technique, 3D data could be recorded and thus would give a better comprehension on the ongoing

investigation (Vasilescu et al., 2005; Campos and Codina, 2015). However, though the AUV technology had been developed since 1960's, researchers and engineers are still struggling to achieve the ultimate swimming performance under the conventional design AUV which is trading off the speed and manoeuvrability of the AUV (Roper et al., 2010). Furthermore, for a small scale sensing AUV which has limited space for energy supply means shortage of operation time. Another concern is the noise from the conventional electric motor is unnecessary. All these constraints had shifted the researchers to the out-of-the-box solution; by getting the inspiration from the nature for design outcome and promoting new actuation techniques (Shi et al., 2013).

Naturally, aquatic animals such as fish, squid and eels are excellent swimmers with high propulsion efficiency in term of both speed and manoeuvrability (Yu et al., 2005). Without rotating propeller, fish for instance manages to move at fast speed (up to 65mph for sailfish) and able to accelerate at difficult angle either to catching its prey or escaping away from its predators (Hingham, 2007). Besides, those aquatic animals manage to move in near silent motion. Ability to move stealthily is a vital characteristic for predator fish. In order to achieve the optimum propulsion efficiency at high manoeuvrability degree and lower drag, researchers had imitated these aquatic animal swimming principles in their AUV design (Chu et al., 2012). This non conventional AUV is known as bio-inspired or biomimetic AUV. In general, there are three main classifications for aquatic animal swimming mechanism which are;

- i. Oscillating
- ii. Undulatory
- iii. Jet propulsion

There are few subcategories between the oscillating and undulatory swimming mechanism or propulsion system as depicted in Figure 1.1 (Colgate and Lynch, 2004).

Almost all aquatic vertebrates such as fish, eels and quite large number of reptile species such as snake, crocodile and iguana utilize oscillating and undulatory swimming mechanics. Only few invertebrates such as squid, jellyfish, octopus and nautilus apply the water jet locomotion. Unlike the oscillating and undulatory swimming mechanism, the water jet propulsion is based on impulse.

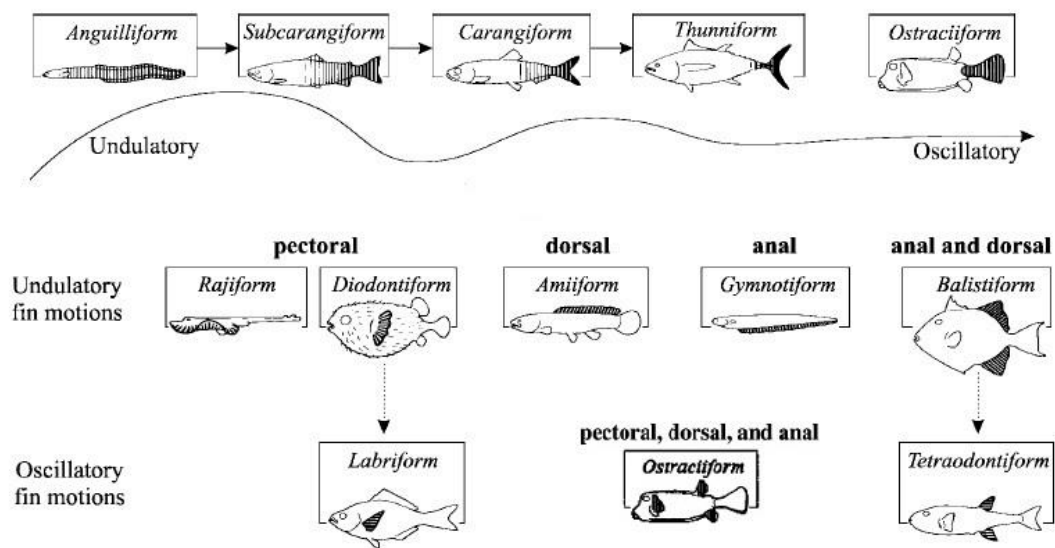


Figure 1.1: Classification of Swimming Mechanism (Colgate and Lynch, 2004)

This impulse is generated from pressurized fluid. Currently, most of the small scale water jet propulsion system is driven by electric motor. The obvious difference between the squid water jet mechanism and the motor powered water jet mechanism is the fluid compression technique. The squid generates water jet pressure using body contraction while the motor powered water jet applies rotary blade compression without body deformation. The utilization of rotary blade compression in commercial thrusters generates noise while the blade propeller induces cavitation in most of the condition and would be harmful for underwater creatures (Wang et al., 2011). The

electric motor itself, contribute unnecessary load. Body contraction water jet which is applied by the squid, compresses the fluid by reducing the mantle volume. This contraction is not a continuous process but it is an intermittent process. Thus, the contraction frequency has significant influence on the thrust efficiency. There are few option of actuators that can be utilized to perform the intermittent contraction. In addition to the contraction frequency, contraction force, water inlet and water outlet opening are another few parameters that must be considered to achieve the optimum thrust efficiency.

Hence, in this research the main goal is to developed contractile water jet thruster (CWJT) and conduct parametrical studies to investigate its performance as a thruster for small AUV. A suitable actuator which is more silent, light and compatible to the sensing measurement condition will be adapted. Based on preliminary studies, there are few options of actuators that could be utilized to substitute the fluid compression techniques which is driven by blade – motor integration. The potential actuators would be pneumatic based actuators and smart material actuators. Though the air is compressible and the actuators could be miniaturized, a complete pneumatic system require air reservoir, compressor and control valve which are too bulky for small scale AUV (Nishioka et al., 2011). Smart material actuators seems likely to fit in the actuation system. However, there are numbers of smart materials with various actuation characteristics and input requirements (Mikhrafi et al., 2007).

Basically, smart material is a man-made material that has one or more properties that is being changed due to external inputs such as electric, electromagnetic fields and light (Chopra, 2002). This characteristics had made smart material as an option to fabricate actuators and artificial muscle. Though there is no specific category for this smart material actuators yet, this actuators could be recognized by its based

materials, which are metal based, ceramic based and polymer based. Shape Memory Alloys (SMA) is one example for metal based smart material and piezoelectric material is a kind of ceramic based smart material. Dielectric elastomer (DE), Conducting Polymers and Ionic Polymer Metal Composite (IPMC) are few examples for polymer based smart materials. Based on the requirement, IPMC had been selected as the potential actuator for the CWJT. IPMC requires low driving voltage, flexible and able to work underwater (Shahinpoor and Kim, 2001). However, the main challenge for this research is mainly comes from the limitation of IPMC whereby the actuation force is between 1.0 gf and 8.0 gf per actuator, depending on the dimensional geometry (Shahinpoor and Kim, 2001). The research works would involve the design and development of CWJT using smart material actuator and investigating the water jet generation performance at different inputs.

## **1.2 Problem Statement**

Currently most of the commercial thruster available in the market for AUV is developed based on electric motor powered rotary blade. The combination of electric motor and the rotary blade along with batteries requires a rigid and stiff AUV body structure to support those items. Basically, rotary thruster produces thrust in one straight direction which represents one axis of motion. Generally, there are three axis of motions for AUV locomotion which are forward – backward motion or surge, upward – downward motion or heave and right – left motion or sway (Benetazzo et al. 2015). Therefore, to perform these motions AUV will be equipped with at least three thrusters. Rotational motion at every axis which are the roll, pitch and yaw requires another three thrusters. Though this thrusters increases the manoeuvrability degree of